

# Single Spin Asymmetry Scaling in the Forward Rapidity Region at RHIC

Zhong-Bo Kang<sup>1,\*</sup> and Feng Yuan<sup>2,1,†</sup>

<sup>1</sup>*RIKEN BNL Research Center, Brookhaven National Laboratory, Upton, NY 11973, USA*

<sup>2</sup>*Nuclear Science Division, Lawrence Berkeley National Laboratory, Berkeley, CA 94720, USA*

## Abstract

We investigate the scaling properties in inclusive hadron production and the associated single transverse spin asymmetry in the forward rapidity region at RHIC. We find that the spin-averaged experimental data in both  $pp$  and  $dAu$  collisions demonstrates a transverse-momentum-dependent geometric scaling. We introduce the transverse momentum dependent Collins fragmentation function to study the scaling of the single transverse spin asymmetries. The general feature of the scaling analysis is consistent with the experimental observations, in particular, for the transverse momentum dependence of the spin asymmetries at RHIC energy. We further propose to probe the saturation scale of nucleus by measuring the spin asymmetry normalized by that in  $pp$  scattering at low transverse momentum.

PACS numbers: 12.38.Bx, 13.85.Ni, 13.88.+e, 24.85.+p

---

\* zkang@bnl.gov

† fyuan@lbl.gov

## I. INTRODUCTION

Since its operation, the forward rapidity region in  $pp$  and  $dAu$  collisions at the Relativistic Heavy Ion Collider (RHIC) has provided important opportunities to study novel hadronic physics phenomena, from the single transverse spin asymmetry (SSA) in  $pp$  collisions [1–4] to the small- $x$  gluon saturation in  $dAu$  collisions [5–8]. Both physics has attracted great attentions in the last few years.

The nuclear suppression observed in hadron production in the forward rapidity region in  $dAu$  collisions at RHIC has been interpreted as the consequence of the saturation physics at small- $x$  [9–14]. An effective theory of the color-glass-condensate (CGC) has been applied to describe these phenomena [15]. Alternative approaches have also been proposed [16–19]. Meanwhile the large single transverse spin asymmetries in  $pp$  collisions found at RHIC have been studied from various approaches [20, 21], while the underlying mechanism remains unclear [22]. In this paper, we will extend the CGC formalism to include the spin effects, in particular, in the fragmentation process. Early attempts have been reported in Ref. [23], where they focused on the spin dependent quark distribution contribution.

One important aspect in the context of the color-glass-condensate is the so-called geometric scaling [24, 25]. This is better understood as that the unintegrated gluon distribution  $N_F(x, q_\perp)$  can be written as a single function of  $q_\perp^2/Q_s^2(x)$  with  $Q_s(x)$  the saturation scale. As a result, the structure function of deep inelastic scattering can be expressed as a single function of  $\tau = Q^2/Q_s^2$  with  $Q$  the virtuality of the exchanged photon [25]. It is remarkable that the experimental data from HERA support this geometric scaling. Since then, this idea has been applied to many hadronic processes involving small- $x$  parton distributions, including some experimental data relevant to the forward region at RHIC.

In the forward rapidity region of  $pp$  (or  $pA$ ) collisions at high energy, the incoming parton from the projectile scatters on the target. Because of high density of the partons from the target at small  $x$  (or in large nucleus), this parton goes through multiple scattering before it fragments into the final state hadron. The CGC formalism takes into account these multiple interaction effects in a systematic manner. In particular, the quantum evolution at small- $x$  in this formalism has been well established and plays a very important role to understand the suppression phenomena observed at RHIC [26].

We further introduce the transverse momentum dependence in the fragmentation functions to understand the single transverse spin asymmetries by introducing the spin-dependent fragmentation function - the Collins function [27]. Previous model studies have claimed that this effect is too small to make any significant contribution to the SSA in forward hadron production in  $pp$  collisions [28]. However, we will find that the CGC formalism provides a simple factorized form for the spin-dependent cross section, from which we find that the Collins mechanism indeed plays an important role. Of course, the limitation of the current knowledge of the quark transversity distribution and the Collins fragmentation function do not allow us to make reliable predictions. However, from the positivity bounds of both functions, we find that it is possible to explain the large single spin asymmetries in hadron production observed by the experiments at RHIC.

The rest of this paper is organized as follows. In Sec. II, we analyze the inclusive hadron production in the forward rapidity region in  $pp$  and  $pA$  collisions following the CGC approach. We will show that the experimental data from RHIC demonstrates a transverse momentum dependent geometric scaling for both  $pp$  and  $dAu$  collisions. In Sec. III, we introduce the transverse momentum dependence in the fragmentation process to understand

the single spin asymmetries in  $pp$  collisions. In particular, the transverse momentum dependence of  $A_N$  indicates the importance of details in the hadronization. We conclude our paper in Sec. IV.

## II. TRANSVERSE MOMENTUM DEPENDENT GEOMETRIC SCALING

In the forward rapidity region, the hadron production in  $pp$  and  $pA$  collisions at high energy is dominated by the valence quark and gluon from the projectile. The energetic parton penetrates in the nucleon (nucleus) target with multiple scattering and then fragments into the final state hadron. We follow the CGC approach to study the differential cross section of hadron production  $p + p(\text{or } A) \rightarrow h + X$  in the forward rapidity region [13, 26],

$$\frac{d\sigma}{dy_h d^2 P_{h\perp}} = \frac{K}{(2\pi)^2} \int_{x_F}^1 \frac{dz}{z^2} x_1 q(x_1) N_F(x_2, k_\perp = P_{h\perp}/z) D_{h/q}(z), \quad (1)$$

where  $K$  is a possible  $K$ -factor to absorb the higher order corrections,  $x_F = P_{h\perp}/\sqrt{s} \exp(y_h)$ , and  $x_1 = x_F/z$  is the momentum fraction of the projectile carried by the incoming quark,  $z$  the momentum fraction of the quark carried by the final state hadron,  $x_2 = x_1 \exp(-2y_h)$  is the momentum fraction of the target participating in the hard scattering. We have also suppressed the scale dependence in various factors in the above formula, for which the precise forms will depend on the next-to-leading order perturbative corrections.

$N_F(x_2, k_\perp)$  is the unintegrated gluon distribution, and is given by the two-dimensional Fourier transform of the imaginary part of the forward dipole-target scattering amplitude in the fundamental representation:

$$N_F(x_2, k_\perp) = \int d^2 r e^{-ik_\perp \cdot r} [1 - \mathcal{N}_F(r, Y = \ln(x_0/x))], \quad (2)$$

with  $r$  the dipole size. The characteristic feature of  $\mathcal{N}_F(r, Y)$  is its “geometric scaling”, i.e.,  $\mathcal{N}_F(r, Y)$  only depends on the dimensionless quantity  $r^2 Q_s^2(x)$  [24, 25]. Thus its Fourier transform has “geometric scaling”:  $k_\perp^2 N_F(x_2, k_\perp)$  depends only on the dimensionless ratio  $k_\perp^2/Q_s^2(x)$ . This property will manifest itself in the differential cross section of hadron production as we will show below.

For the large- $x$  quark and gluon distribution, an important power counting can be applied to study the general behavior for the differential cross section of the above process [29, 30]. In particular, for the region where the quark distribution dominates, we have  $q(x) \sim (1-x)^3$ . Furthermore, fragmentation function also has power counting rule,  $D_{h/q}(z) \sim (1-z)$ , where the power behavior comes from the current parameterization of the fragmentation function for the charged and neutral pions [31]<sup>1</sup>. Combining the above power counting analysis, we obtain the following power behavior for the differential cross section,

$$P_{h\perp}^2 \frac{d\sigma}{dy_h d^2 P_{h\perp}} = (1-x_F)^5 \mathcal{F} \left( \frac{P_{h\perp}^2}{Q_s^2(x_2)} \right), \quad (3)$$

where the saturation scale  $Q_s$  depends on the target and the momentum fraction  $x_2$  carried by the gluon. The geometric scaling (as a function of  $P_{h\perp}^2/Q_s^2$  only) comes from the geometric scaling of the unintegrated gluon distribution for  $k_\perp^2 N_F(x, k_\perp)$  as mentioned above.

<sup>1</sup> The original power counting would predict  $(1-z)^2$  behavior for the spin-averag fragmentation functions [30]. This would lead to a power behavior of  $(1-x_F)^6$  instead of  $(1-x_F)^5$  in Eq. (3). The current data in Fig. 1 can be described by both parameterizations. Future experimental data at very forward region shall be able to distinguish them.

Similar geometric scaling for inclusive hadron production at central rapidity has been observed in [32, 33], where it is the differential cross section alone exhibits the geometric scaling. On the contrary, we have to multiply a factor of  $P_{h\perp}^2$  to the differential cross section to show the geometric scaling. The geometric scaling derived in [32, 33] relies on the  $k_T$ -factorization (implicitly), and both incoming hadrons contribute to the saturation effects in the particle production at mid-rapidity, where the saturation scales from the two incoming hadrons are in the same order at mid-rapidity. However, in our analysis, we have a dilute projectile scattering on a dense target, where the saturation only comes from the dense target and the geometric scaling is manifest in the first place. Of course, as a result, the differential cross section has to be multiplied by a factor of  $P_{h\perp}^2$  to demonstrate the geometric scaling.

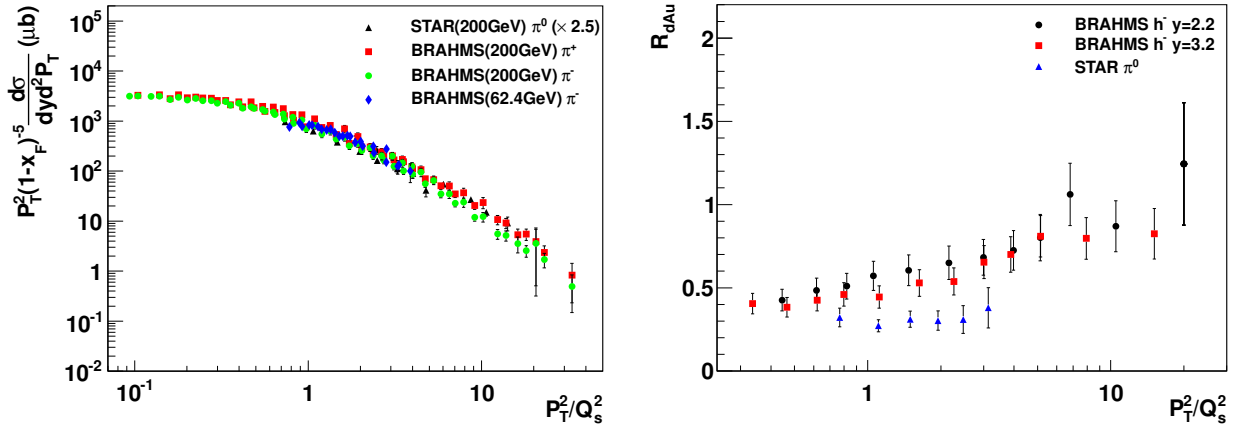


FIG. 1. Geometric scaling of the differential cross sections (left) and the nuclear modification factor  $R_{dAu}$  (right) plotted as a function of  $P_{h\perp}^2/Q_s^2$ . Data are from BRAHMS [5] and STAR [6] Collaborations at RHIC.

In Fig. 1, we plot the RHIC data in  $pp$  collisions the differential cross section,

$$(1 - x_F)^{-5} P_{h\perp}^2 \frac{d\sigma(pp \rightarrow h + X)}{dy_h d^2 P_{h\perp}} \quad (4)$$

as a function of  $P_{h\perp}^2/Q_s^2(x_2)$ , where  $x_2$  is calculated as  $x_2 = P_{h\perp}^2/(x_1 s) \approx P_{h\perp}^2/(x_F S)$ , and the saturation scale  $Q_s^2(x_2) = Q_0^2(x_0/x_2)^\lambda$  with  $Q_0 = 1$  GeV,  $x_0 = 3 \cdot 10^{-4}$ , and  $\lambda = 0.28$  [24]. In this plot, we have included the data for  $\pi^\pm$  from BRAHMS collaboration [5] and  $\pi^0$  from the STAR collaboration [6] at  $\sqrt{s} = 200$  GeV.  $\pi^\pm$  data are from two rapidity bins  $y_h = 2.95$  and  $y_h = 3.3$ , whereas those for  $\pi^0$  cover  $y_h = 3.3, 3.8, 4.0$ . We have also included data for  $\pi^-$  production at lower energy  $\sqrt{s} = 62.4$  GeV from BRAHMS at  $y_h = 2.7$  and  $y_h = 3.3$  [5]. For  $\pi^0$  production, we have multiplied a factor 2.5, which is consistent with the overall  $K$ -factor  $K \sim 0.4$  found in [13]. From this plot, we see clearly that the hadron production in the forward rapidity region demonstrates the geometric scaling.

It is also interesting to check the geometric scaling when we compare the  $pA$  and  $pp$  collisions in the forward rapidity region [34]. Here, the nuclear modification factor  $R_{pA}$  is measured,

$$R_{pA} = \frac{dN^{pA \rightarrow h+X} / dy_h d^2 P_{h\perp}}{N_{coll} dN^{pp \rightarrow h+X} / dy_h d^2 P_{h\perp}}, \quad (5)$$

where  $N_{coll}$  represents the number of binary collisions in the selected nucleon-nucleus scattering. Many factors cancel out in the above ratio. Therefore, according to Eq. (3) we will have the following geometric scaling behavior,

$$R_{pA} = \mathcal{R}_b \left( \frac{P_{h\perp}^2}{Q_s^2(x_2)} \right), \quad (6)$$

where again the saturation scale  $Q_s$  depends on the momentum fraction of the nucleus target involved in the scattering process and is determined by the kinematics of  $P_{h\perp}$  and rapidity  $y_h$ . In the above equation the subscript  $b$  indicates that the ratio also depends on the centrality of the collision, which determines the change of the saturation scale from  $pp$  collision to  $pA$  collision at a given impact parameter. Of course, the magnitude  $\mathcal{R}$  depends on the overall normalization as well, including the parameter  $N_{coll}$ .

As an illustration, we plot the  $R_{dAu}$  for hadron production at  $\sqrt{s} = 200$  GeV in the forward rapidity region, where we include the BRAHMS data for the negative charged hadron  $h^-$  at two rapidities:  $y_h = 2.2$  and  $y_h = 3.3$ , and the STAR data for neutral pion at  $y_h = 4.0$ . Clearly, the two rapidity sets from BRAHMS demonstrate the geometric scaling behavior, whereas the STAR data are a little off the scaling curve of the negative charged hadrons. This indicates additional mechanism for very forward hadron suppression in  $dA$  collisions [19]. It will be very interesting to further test this geometric scaling in the future experiments at RHIC and the LHC.

The power behavior for the differential cross section has been observed in various scattering energies, and has been used as a practice to understand the forward hadron production. However, the geometric scaling only appears when we hit the saturation region at small- $x$  of the target. For example, we notice that the forward hadron production at low energy fixed-target experiments does not show the same scaling behavior [35]. This tells us that geometric scaling is not yet reached in these energies, and the production mechanism differs. Similar conclusions have been drawn from the comparison between the RHIC data and those from the previous fixed-target experiments in the collinear factorization approach [36, 37].

### III. SINGLE SPIN ASYMMETRY IN THE FORWARD REGION

In this section, we extend the above formalism to calculate the single spin asymmetry in the forward region. For this purpose, we need to introduce the transverse momentum dependence either in the incoming parton distribution from the projectile (polarized proton) [23] and/or the fragmentation function. Here we concentrate on the contribution from the fragmentation function.

In the forward rapidity, introducing the transverse momentum dependence in the fragmentation function in Eq. (1), we have the spin-averaged differential cross section

$$\frac{d\sigma}{dy_h d^2 P_{h\perp}} = \frac{K}{(2\pi)^2} \int_{x_F}^1 \frac{dz}{z^2} \int d^2 P_{hT} x_1 q(x_1) N_F(x_2, k_\perp) D_{h/q}(z, P_{hT}), \quad (7)$$

where  $P_{hT}$  is the transverse momentum of the final state hadron relative to the fragmenting quark jet, thus the momentum of the final state hadron in Lab frame can be written as:  $\mathbf{P}_{h\perp} \approx z \mathbf{k}_\perp + \mathbf{P}_{hT}$ . On the other hand, the spin-dependent differential cross section for  $p^\uparrow + p(\text{or } A) \rightarrow h + X$  can be written as [38]

$$\frac{d\Delta\sigma}{dy_h d^2 P_{h\perp}} = \frac{K}{(2\pi)^2} \int_{x_F}^1 \frac{dz}{z^2} \int d^2 P_{hT} I(S_\perp, P_{hT}) x_1 h(x_1) N_F(x_2, k_\perp) \delta\hat{q}(z, P_{hT}), \quad (8)$$

where  $h(x_1)$  is the quark transversity,  $\delta\hat{q}(z, P_{hT})$  is the Collins function that is related to the Trento convention [39] as:  $\delta\hat{q}(z, P_{hT}) = -H_1^\perp/zM_h$  with  $M_h$  the final-state hadron mass. The azimuthal angle dependence is encoded in  $I(S_\perp, P_{hT})$  and is given by

$$I(S_\perp, P_{hT}) = \epsilon^{\alpha\beta} S_\perp^\alpha \left[ P_{hT}^\beta - \frac{n \cdot P_{hT}}{n \cdot P_J} P_J^\beta \right], \quad (9)$$

where  $\epsilon^{\alpha\beta}$  is the 2-dimensional Levi-Civita tensor with  $\epsilon^{12} = 1$ ,  $n$  is a unit vector along the momentum of the unpolarized hadron, and  $P_J$  is the momentum of the fragmenting quark jet. In the forward rapidity region,  $I(S_\perp, P_{hT})$  can be reduced to the following form,

$$I(S_\perp, P_{hT}) = |S_\perp| |P_{hT}| \sin(\phi_h - \phi_s), \quad (10)$$

where  $\phi_s$  is the azimuthal angle for the spin vector  $S_\perp$  in the Lab frame,  $\phi_h$  is the azimuthal angle of the produced hadron momentum  $P_{h\perp}$  relative to the fragmenting quark jet.

The single transverse spin asymmetry is defined as

$$A_N = \frac{d\Delta\sigma}{dy_h d^2 P_{h\perp}} \bigg/ \frac{d\sigma}{dy_h d^2 P_{h\perp}}. \quad (11)$$

To be consistent with the experimental definition we choose the coordinate system where hadron transverse momentum  $P_{h\perp}$  along  $x$ -direction, the spin vector  $S_\perp$  along  $y$ -direction, and the polarized beam along  $z$ -direction.

Before we present the numeric estimates, we would like to study the generic feature for the single spin asymmetry in the above approach. We will take a simple model for the unintegrated gluon distribution and the Collins fragmentation function to study the transverse momentum behavior of the single spin asymmetry. First, we will examine the single spin asymmetry at relative low transverse momentum at order of the saturation scale:  $P_{h\perp}^2 \sim Q_s^2$ . We know that the unintegrated gluon distribution has saturation behavior at low transverse momentum. As a convenient model, we follow the GBW parameterization [24]

$$N_F(x, q_\perp) \sim \frac{1}{Q_s^2} e^{-q_\perp^2/Q_s^2}, \quad (12)$$

which has geometric scaling. For the fragmentation function we choose a simple Gaussian distribution,

$$D_{h/q}(z, p_\perp) \sim \frac{1}{\Delta^2} e^{-p_\perp^2/\Delta^2}, \quad (13)$$

where  $\Delta^2$  represents the width of the transverse momentum dependence in the fragmentation function. By performing the transverse momentum integration in Eq. (7), we will find that the spin-averaged cross section has the following transverse momentum behavior,

$$\frac{d\sigma}{dy_h d^2 P_{h\perp}} \sim \frac{1}{Q_s^2 + \Delta^2} e^{-P_{h\perp}^2/(Q_s^2 + \Delta^2)}, \quad (14)$$

where we limit the above results at small transverse momentum region of order of  $Q_s$ . If the saturation scale  $Q_s$  is much larger than the transverse momentum width  $\Delta$  in the fragmentation function, we will find that the transverse momentum dependence in the fragmentation function does not change the geometric scaling discussed in the last section.

Now we turn to the spin-dependent differential cross section. For the Collins function, we assume it also has a Gaussian form [38],

$$\delta\hat{q}(z, p_\perp^2) \sim \frac{1}{(\Delta^2 - \delta^2)^{3/2}} e^{-p_\perp^2/(\Delta^2 - \delta^2)}, \quad (15)$$

with a slight difference in the Gaussian width  $\Delta^2 - \delta^2$  to satisfy the positive bound. Substituting the above equation to the differential cross section formula in Eq. (8), one obtains,

$$\frac{d\Delta\sigma}{dy_h d^2P_{h\perp}} \propto \frac{P_{h\perp} \sqrt{\Delta^2 - \delta^2}}{(Q_s^2 + \Delta^2 - \delta^2)^2} e^{-\frac{P_{h\perp}^2}{Q_s^2 + \Delta^2 - \delta^2}}, \quad (16)$$

From the above results, we find that the single spin asymmetry behaves as,

$$\begin{aligned} A_N(P_{h\perp}) &\propto \frac{P_{h\perp}(Q_s^2 + \Delta^2)\sqrt{\Delta^2 - \delta^2}}{(Q_s^2 + \Delta^2 - \delta^2)^2} e^{-\frac{P_{h\perp}^2}{Q_s^2 + \Delta^2 - \delta^2} + \frac{P_{h\perp}^2}{Q_s^2 + \Delta^2}} \\ &\approx \frac{P_{h\perp}\Delta}{Q_s^2 + \Delta^2} e^{-\frac{\delta^2 P_{h\perp}^2}{(Q_s^2 + \Delta^2)^2}} \\ &\approx \frac{P_{h\perp}\Delta}{Q_s^2} e^{-\frac{\delta^2 P_{h\perp}^2}{(Q_s^2)^2}}, \end{aligned} \quad (17)$$

where we have made reasonable assumptions:  $Q_s^2 \gg \Delta^2 \gg \delta^2$ . The above result indicates that the asymmetry vanishes when  $P_{h\perp} \rightarrow 0$ , and it also depends on the transverse momentum width in the fragmentation function. Certainly, if there is no transverse momentum dependence, the whole effects will vanish. Furthermore, the spin asymmetry also decreases with the saturation scale. This is because the fragmentation effect is suppressed if we increase the saturation scale (see also Eq. (14)). From the above simple analysis, we find that the spin asymmetry in general will have broader distribution as a function of  $P_{h\perp}$ .

Moreover, it is interesting to note that the double ratio of the spin asymmetries between  $p^\uparrow A$  and  $p^\uparrow p$  scatterings scales as

$$\left. \frac{A_N^{pA \rightarrow h}}{A_N^{pp \rightarrow h}} \right|_{P_{h\perp}^2 \ll Q_s^2} \approx \frac{Q_{sp}^2}{Q_{sA}^2} e^{\frac{P_{h\perp}^2 \delta^2}{Q_{sp}^4}}, \quad (18)$$

at small transverse momentum, where we have assumed that the saturation scale for nucleus is much larger than that for the nucleon at the same kinematics. This is the most interesting result from the scaling analysis. The ratio of the spin asymmetry is inversely proportional to the saturation scale in the limit of  $P_{h\perp} \rightarrow 0$ . This can be used as an important probe for the saturation scale of the gluon distribution in the nuclei target.

Similarly, we can estimate the large transverse momentum behavior for the spin asymmetries, where the unintegrated gluon distribution behaves as

$$N_F(x, q_\perp) \sim \frac{Q_s^2}{q_\perp^4}. \quad (19)$$

If we still assume that the fragmentation function can be parametrized as a Gaussian form, we will find out,

$$A_N(P_{h\perp}) \propto \frac{2P_{h\perp}\sqrt{\Delta^2 - \delta^2}}{P_{h\perp}^2 + 4\Delta^2}, \quad (20)$$

where the factor 4 comes from the power of the unintegrated gluon distribution at large transverse momentum. The asymmetry decreases as  $1/P_{h\perp}$  at large transverse momentum as expected. However, the rate of the decreasing is strongly affected by the relative size between  $P_{h\perp}^2$  and  $\Delta^2$ . This additional  $4\Delta^2$  modification is slightly different from the usual  $1/P_{h\perp}$  power counting results [20]. It comes from the effects of the transverse momentum dependent fragmentation function in the spin-averaged cross section which was neglected previously [20].

Furthermore, we notice that the saturation scale dependence cancels out between the spin-averaged and the spin-dependent cross sections, and the asymmetry does not depend on the saturation scale. As a consequence, the double ratio will approach

$$\left. \frac{A_N^{pA \rightarrow h}}{A_N^{pp \rightarrow h}} \right|_{P_{h\perp}^2 \gg Q_s^2} \approx 1. \quad (21)$$

The above results are very interesting observations, and it will be important to test these predictions in the future experiments [41].

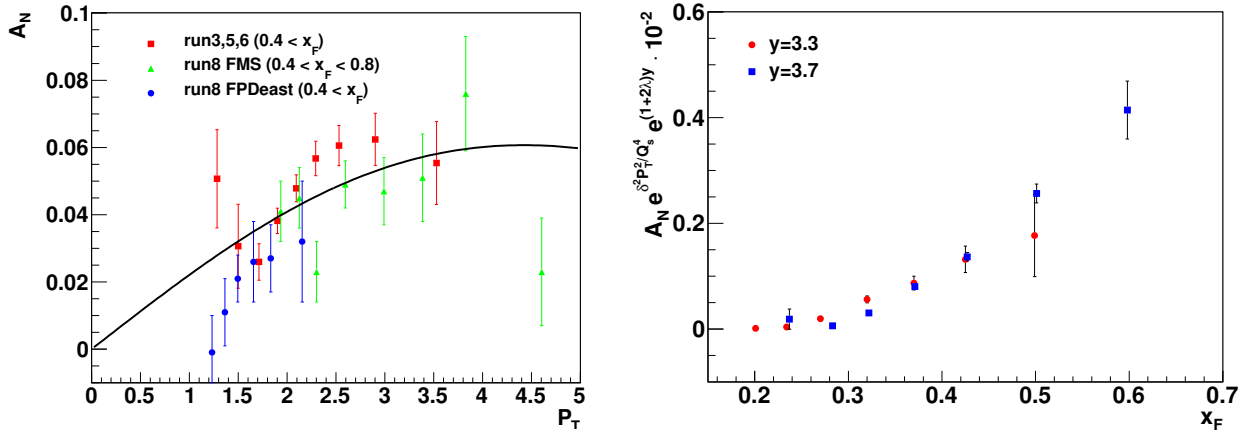


FIG. 2. Left:  $P_{h\perp}$ -dependence of the single spin asymmetry. We use Eq. (17) to fit the STAR experimental data [2, 42]. Right: We plot  $A_N e^{\delta^2 P_{h\perp}^2 / Q_s^4} e^{(1+2\lambda)y}$  as a function of  $x_F$  - the generalized  $x_F$ -scaling for the single spin asymmetry according to Eq. (23). We have chosen  $\delta = 0.16$  GeV to demonstrate the scaling. The data is from STAR [2].

Comparing Eqs. (17) and (20), we find that the maximum of the single spin asymmetry will be at  $P_{h\perp}^2 \sim Q_s^4 / \delta^2$ . Since  $\delta^2$  is a small number, we would find that the spin asymmetry drops at a relatively large transverse momentum, which seems to be consistent with the observations at RHIC experiments [2, 40]. In Fig. 2 (left), we show the comparison of Eq.(17) with the experimental data from the STAR collaboration [2, 42], where we have chosen  $Q_s^2 \approx 1.0$  GeV<sup>2</sup>, which is roughly the average saturation scale in this experimental kinematic region.  $\delta \approx 0.16$  GeV is adjusted to fit the experimental data. Although the normalization of the asymmetry depends on  $\Delta^2$  and the size of the Collins effect, including the quark transversity distribution and the Collins fragmentation function, the transverse momentum dependence from our general analysis is consistent with the experimental data.

Meanwhile, from Eq. (17) and realizing  $P_{h\perp} = x_F \sqrt{S} e^{-y_h}$ , we find

$$A_N \sim x_F^{(1+\lambda)} e^{-(1+2\lambda)y_h} e^{-\delta^2 P_{h\perp}^2 / Q_s^4} \mathcal{F}(x_F), \quad (22)$$



where  $\mathcal{F}(x_F)$  represents any additional  $x_F$  dependence for the single spin asymmetry. Therefore, the following quantity

$$A_N e^{\delta^2 P_{h\perp}^2 / Q_s^4} e^{(1+2\lambda)y_h} \sim x_F^{(1+\lambda)} \mathcal{F}(x_F), \quad (23)$$

will be a universal function of  $x_F$ , independent of the rapidities. In Fig. 2 (right), we plot STAR  $\pi^0$  single spin asymmetry data for the quantity defined in Eq. (23) as a function of  $x_F$  for two rapidities  $y_h = 3.3$  and  $y_h = 3.7$ . We find that for relatively small  $\delta \lesssim 0.2$  GeV (which is consistent with our approximation), the data seem to be consistent with the  $x_F$ -scaling. It will be interesting to test this scaling in the future experiments. Note that we derive this interesting scaling purely from the fragmentation process, but it could also come from the distribution function (Sivers function) in the polarized nucleon [20]. However, the complicated structure for the Sivers function makes such a study nontrivial [22].

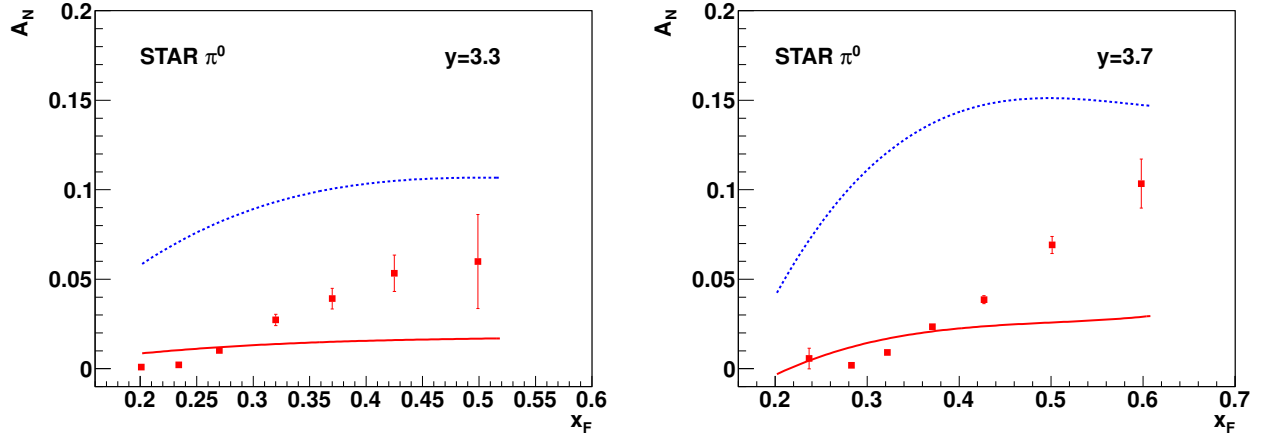


FIG. 3. The comparison with the STAR experimental data at  $\sqrt{s} = 200$  GeV for rapidity  $y_h = 3.3$  (left) and  $y_h = 3.7$  (right). The solid lines are using the transversity from [43, 44] and the Collins function from [38, 44]. The dashed curves are the upper bound as explained in the text.

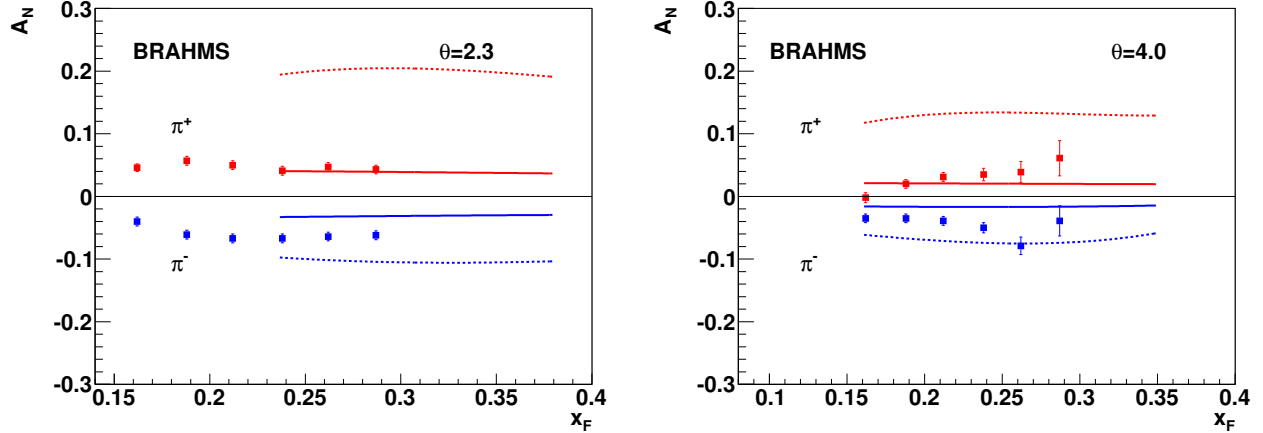


FIG. 4. The comparison with BRAHMS experimental data at  $\sqrt{s} = 200$  GeV. The curves are the same as explained in Fig. 3.

Let us now come back to make some numerical estimates for the single spin asymmetry. For this purpose, we will use the unintegrated gluon distribution in Ref. [13], which comes from solving Balitsky-Kovchegov equation with running-coupling corrections. We will choose the quark transversity in [43, 44], and adopt the transverse momentum dependent unpolarized fragmentation function and Collins function in [38, 44],

$$D_{h/q}(z, P_{hT}) = \frac{1}{\pi \langle p_{\perp}^2 \rangle} e^{-P_{hT}^2 / \langle p_{\perp}^2 \rangle} D_{h/q}(z), \quad (24)$$

$$\delta \hat{q}(z, P_{hT}) = \frac{2}{(\pi \langle p_{\perp}^2 \rangle)^{3/2}} e^{-P_{hT}^2 / \langle p_{\perp}^2 \rangle} \delta \hat{q}^{(1/2)}(z), \quad (25)$$

where  $\langle p_{\perp}^2 \rangle = 0.2 \text{ GeV}^2$ , and  $\delta \hat{q}^{(1/2)}(z)$  is the so-called half-moment of the Collins function given in [38, 44]. The numerical estimates for the single spin asymmetry of  $\pi^0$  are shown in Fig. 3 as solid lines, and also compared with the experimental data from STAR collaboration [2]. Similar comparison for the charged pions are shown in Fig. 4 with the experimental data from BRAHMS collaboration [4].

From these plots, it seems that the predictions are below the experimental data. However, it is important to keep in mind that there are uncertainties in both the quark transversity distribution and the Collins fragmentation function. For example, the quark transversity is constrained using experimental data from HERMES collaboration, only up to  $x \lesssim 0.3$  [45], thus we are lacking of information on the transversity in the interested region at RHIC forward direction  $x > 0.3$ . The situation for the Collins function is slightly better since we have complimentary information from both semi-inclusive deep inelastic scattering at HERMES [45] and  $e^+e^-$  collisions at BELLE [46]. But one still needs to understand how to incorporate the evolution of the Collins function, which will affect the Gaussian approximation and the Gaussian width used above [47]. Realizing the limitation of the current knowledge for both quark transversity and Collins function, we will set up a bound for the single spin asymmetry by using the positivity bounds for both functions.

For transversity, we saturate the Soffer bound [48], which is derived from positivity [49]. Following Ref. [28], we choose

$$h_u(x) = \frac{1}{2} [u(x) + \Delta u(x)], \quad h_d(x) = -\frac{1}{2} [d(x) + \Delta d(x)], \quad (26)$$

where  $\Delta q(x)$  is the helicity distribution function,  $h_q(x)$  is the quark transversity. For the Collins function, we have

$$P_{hT} \delta \hat{u}^{\pi^+}(z, P_{hT}) = -D_u^{\pi^+}(z, P_{hT}), \quad (27)$$

$$P_{hT} \delta \hat{d}^{\pi^+}(z, P_{hT}) = D_d^{\pi^+}(z, P_{hT}). \quad (28)$$

where the signs are chosen such that we have the maximum single spin asymmetry for the charged pions [28]. For  $\pi^0$ , we rely on the isospin symmetry. In Figs. 3 and 4, the dashed lines are the upper bound for the single spin asymmetries. From these plots, we see the Collins mechanism in CGC formalism is large enough to explain the observed asymmetries. If the Collins mechanism is the dominant contribution to the single spin asymmetries [22], one should be able to extract the quark transversity and Collins function by using the RHIC data.

## IV. SUMMARY

We study the scaling properties in the inclusive single hadron production and the associated single transverse spin asymmetries in the forward rapidity region at RHIC. For the spin-averaged differential cross sections in both  $pp$  and  $pA$  collisions, we find a transverse momentum dependent geometric scaling. These scalings are clearly seen in the spin-averaged experimental data in both  $pp$  and  $dAu$  collisions. We further introduce the transverse momentum dependence in the fragmentation function to investigate the scaling of the single transverse spin asymmetry associated with the Collins mechanism. The general behavior of the transverse momentum dependence of the single spin asymmetry is consistent with the trend observed in the experiments at RHIC. We also find that the double ratio of the spin asymmetries in  $pA$  and  $pp$  collisions is inversely proportional to the saturation scale in the limit of  $P_{h\perp} \rightarrow 0$ . This can be used to probe the saturation scale in the nucleus by measuring the spin asymmetry normalized by that in  $pp$  scattering at low transverse momentum.

With the limited knowledge for the relevant functions - quark transversity and Collins function, we set up an upper bound for the single spin asymmetry. We find that the bound is certainly large enough to explain the experimental data at RHIC.

## ACKNOWLEDGMENTS

We thank L. McLerran and R. Venugopalan for helpful discussions, and thank J. L. Albacete for providing us their unintegrated gluon distribution used in our numerical estimate. We also thank L. Bland, L. Eun, S. Heppelmann, J. H. Lee, A. Ogawa, and F. Videbaek for the discussions on the experimental data. This work was supported in part by the U.S. Department of Energy under Grant No. DE-AC02-05CH11231. We are grateful to RIKEN, Brookhaven National Laboratory, and the U.S. Department of Energy (Contract No. DE-AC02-98CH10886) for supporting this work.

- 
- [1] J. Adams *et al.* [STAR Collaboration], Phys. Rev. Lett. **92**, 171801 (2004) [arXiv:hep-ex/0310058].
  - [2] B. I. Abelev *et al.* [STAR Collaboration], Phys. Rev. Lett. **101**, 222001 (2008) [arXiv:0801.2990 [hep-ex]].
  - [3] I. Arsene *et al.* [BRAHMS Collaboration], Phys. Rev. Lett. **101**, 042001 (2008) [arXiv:0801.1078 [nucl-ex]].
  - [4] J. H. Lee and F. Videbaek [BRAHMS Collaboration], AIP Conf. Proc. **915**, 533 (2007).
  - [5] I. Arsene *et al.* [BRAHMS Collaboration], Phys. Rev. Lett. **93**, 242303 (2004) [arXiv:nucl-ex/0403005]; F. Videbaek [BRAHMS Collaboration], talk presented at “2007 Annual Fall Meeting of the APS Division of Nuclear Physics”, Newport News, Virginia, Oct. 2007.
  - [6] J. Adams *et al.* [STAR Collaboration], Phys. Rev. Lett. **97**, 152302 (2006) [arXiv:nucl-ex/0602011].
  - [7] E. Braidot [STAR Collaboration], arXiv:1005.2378 [hep-ph].
  - [8] A. Adare *et al.* [PHENIX Collaboration], arXiv:1105.5112 [nucl-ex].

- [9] D. Kharzeev, Y. V. Kovchegov and K. Tuchin, Phys. Rev. D **68**, 094013 (2003) [arXiv:hep-ph/0307037]; D. Kharzeev, Y. V. Kovchegov and K. Tuchin, Phys. Lett. B **599**, 23 (2004) [arXiv:hep-ph/0405045].
- [10] J. L. Albacete, N. Armesto, A. Kovner, C. A. Salgado and U. A. Wiedemann, Phys. Rev. Lett. **92**, 082001 (2004) [arXiv:hep-ph/0307179].
- [11] D. Boer, A. Utermann and E. Wessels, Phys. Rev. D **77**, 054014 (2008) [arXiv:0711.4312 [hep-ph]].
- [12] R. Baier, Y. Mehtar-Tani and D. Schiff, Nucl. Phys. A **764**, 515 (2006) [arXiv:hep-ph/0508026].
- [13] J. L. Albacete and C. Marquet, Phys. Lett. B **687**, 174 (2010) [arXiv:1001.1378 [hep-ph]].
- [14] J. L. Albacete and C. Marquet, Phys. Rev. Lett. **105**, 162301 (2010) [arXiv:1005.4065 [hep-ph]].
- [15] See, for example, E. Iancu and R. Venugopalan, arXiv:hep-ph/0303204; H. Weigert, Prog. Part. Nucl. Phys. **55**, 461 (2005) [arXiv:hep-ph/0501087]; F. Gelis, E. Iancu, J. Jalilian-Marian and R. Venugopalan, arXiv:1002.0333 [hep-ph]; and references therein.
- [16] J. W. Qiu and I. Vitev, Phys. Lett. B **632**, 507 (2006) [arXiv:hep-ph/0405068].
- [17] V. Guzey, M. Strikman and W. Vogelsang, Phys. Lett. B **603**, 173 (2004) [arXiv:hep-ph/0407201].
- [18] B. Z. Kopeliovich, J. Nemchik, I. K. Potashnikova, M. B. Johnson and I. Schmidt, Phys. Rev. C **72**, 054606 (2005) [arXiv:hep-ph/0501260].
- [19] L. Frankfurt and M. Strikman, Phys. Lett. B **645**, 412 (2007) [arXiv:nucl-th/0603049].
- [20] C. Kouvaris, J. W. Qiu, W. Vogelsang and F. Yuan, Phys. Rev. D **74**, 114013 (2006) [arXiv:hep-ph/0609238]; K. Kanazawa and Y. Koike, arXiv:1104.0117 [hep-ph]; Z. B. Kang, J. W. Qiu, W. Vogelsang and F. Yuan, Phys. Rev. D **78**, 114013 (2008) [arXiv:0810.3333 [hep-ph]]; Z. B. Kang, F. Yuan and J. Zhou, Phys. Lett. B **691**, 243 (2010) [arXiv:1002.0399 [hep-ph]].
- [21] M. Anselmino, M. Boglione and F. Murgia, Phys. Lett. B **362**, 164 (1995) [arXiv:hep-ph/9503290]; M. Boglione, U. D'Alesio and F. Murgia, Phys. Rev. D **77**, 051502 (2008) [arXiv:0712.4240 [hep-ph]]; L. Gamberg and Z. B. Kang, Phys. Lett. B **696**, 109 (2011) [arXiv:1009.1936 [hep-ph]]; Z. B. Kang and J. W. Qiu, Phys. Rev. D **81**, 054020 (2010) [arXiv:0912.1319 [hep-ph]].
- [22] Z. B. Kang, J. W. Qiu, W. Vogelsang and F. Yuan, Phys. Rev. D **83**, 094001 (2011) [arXiv:1103.1591 [hep-ph]].
- [23] D. Boer, A. Dumitru and A. Hayashigaki, Phys. Rev. D **74**, 074018 (2006) [arXiv:hep-ph/0609083].
- [24] K. J. Golec-Biernat and M. Wusthoff, Phys. Rev. D **59**, 014017 (1998) [arXiv:hep-ph/9807513].
- [25] A. M. Stasto, K. J. Golec-Biernat and J. Kwiecinski, Phys. Rev. Lett. **86**, 596 (2001) [arXiv:hep-ph/0007192].
- [26] A. Dumitru, A. Hayashigaki and J. Jalilian-Marian, Nucl. Phys. A **765**, 464 (2006) [arXiv:hep-ph/0506308].
- [27] J. C. Collins, Nucl. Phys. B **396**, 161 (1993) [arXiv:hep-ph/9208213].
- [28] M. Anselmino, M. Boglione, U. D'Alesio, E. Leader and F. Murgia, Phys. Rev. D **71**, 014002 (2005) [arXiv:hep-ph/0408356].
- [29] J. F. Gunion, Phys. Rev. D **10**, 242 (1974); R. Blankenbecler and S. J. Brodsky, Phys. Rev. D **10**, 2973 (1974); G. R. Farrar and D. R. Jackson, Phys. Rev. Lett. **35**, 1416 (1975); G. P. Lepage and S. J. Brodsky, Phys. Rev. D **22**, 2157 (1980).

- [30] S. J. Brodsky, M. Burkardt and I. Schmidt, Nucl. Phys. B **441**, 197 (1995) [arXiv:hep-ph/9401328]; S. J. Brodsky and F. Yuan, Phys. Rev. D **74**, 094018 (2006) [arXiv:hep-ph/0610236].
- [31] S. Kretzer, Phys. Rev. D **62**, 054001 (2000) [arXiv:hep-ph/0003177]; B. A. Kniehl, G. Kramer and B. Potter, Nucl. Phys. B **582**, 514 (2000) [arXiv:hep-ph/0010289]; S. Albino, B. A. Kniehl and G. Kramer, Nucl. Phys. B **725**, 181 (2005) [arXiv:hep-ph/0502188]; M. Hirai, S. Kumano, T. H. Nagai and K. Sudoh, Phys. Rev. D **75**, 094009 (2007) [arXiv:hep-ph/0702250]. D. de Florian, R. Sassot and M. Stratmann, Phys. Rev. D **75**, 114010 (2007) [arXiv:hep-ph/0703242]; Phys. Rev. D **76**, 074033 (2007) [arXiv:0707.1506 [hep-ph]].
- [32] L. McLerran and M. Praszalowicz, Acta Phys. Polon. B **41**, 1917 (2010) [arXiv:1006.4293 [hep-ph]]; Acta Phys. Polon. B **42**, 99 (2011) [arXiv:1011.3403 [hep-ph]].
- [33] P. Tribedy and R. Venugopalan, Nucl. Phys. A **850**, 136 (2011) [arXiv:1011.1895 [hep-ph]].
- [34] N. Armesto, C. A. Salgado and U. A. Wiedemann, Phys. Rev. Lett. **94**, 022002 (2005) [arXiv:hep-ph/0407018].
- [35] D. Lloyd Owen *et al.*, Phys. Rev. Lett. **45**, 89 (1980).
- [36] C. Bourrely and J. Soffer, Eur. Phys. J. C **36**, 371 (2004) [arXiv:hep-ph/0311110].
- [37] D. de Florian and W. Vogelsang, Phys. Rev. D **71**, 114004 (2005) [arXiv:hep-ph/0501258].
- [38] F. Yuan, Phys. Lett. B **666**, 44 (2008) [arXiv:0804.3047 [hep-ph]].
- [39] A. Bacchetta, U. D'Alesio, M. Diehl and C. A. Miller, Phys. Rev. D **70**, 117504 (2004) [arXiv:hep-ph/0410050].
- [40] F. Wei [PHENIX Collaboration], talk presented at “XIX International Workshop on Deep-Inelastic Scattering and Related Subjects (DIS 2011)”, Newport News, Virginia, Apr. 2011.
- [41] STAR decadal plan, [http://www.bnl.gov/npp/docs/STAR\\_Decadal\\_Plan\\_Final\[1\].pdf](http://www.bnl.gov/npp/docs/STAR_Decadal_Plan_Final[1].pdf).
- [42] J. L. Drachenberg [STAR Collaboration], AIP Conf. Proc. **1149**, 517 (2009) [arXiv:0901.2763 [hep-ex]].
- [43] O. Martin, A. Schafer, M. Stratmann and W. Vogelsang, Phys. Rev. D **57**, 3084 (1998) [arXiv:hep-ph/9710300].
- [44] W. Vogelsang and F. Yuan, Phys. Rev. D **72**, 054028 (2005) [arXiv:hep-ph/0507266].
- [45] A. Airapetian *et al.* [HERMES Collaboration], Phys. Rev. Lett. **94**, 012002 (2005) [arXiv:hep-ex/0408013].
- [46] K. Abe *et al.* [Belle Collaboration], Phys. Rev. Lett. **96**, 232002 (2006) [arXiv:hep-ex/0507063]; R. Seidl *et al.* [Belle Collaboration], Phys. Rev. D **78**, 032011 (2008) [arXiv:0805.2975 [hep-ex]].
- [47] A. Idilbi, X. d. Ji, J. P. Ma and F. Yuan, Phys. Rev. D **70**, 074021 (2004) [arXiv:hep-ph/0406302]; S. M. Aybat and T. C. Rogers, arXiv:1101.5057 [hep-ph]; Z. B. Kang, Phys. Rev. D **83**, 036006 (2011) [arXiv:1012.3419 [hep-ph]]; Z. B. Kang, B. W. Xiao and F. Yuan, arXiv:1106.0266 [hep-ph].
- [48] J. Soffer, Phys. Rev. Lett. **74**, 1292 (1995) [arXiv:hep-ph/9409254].
- [49] X. Artru, M. Elchikh, J. M. Richard, J. Soffer and O. V. Teryaev, Phys. Rept. **470**, 1 (2009) [arXiv:0802.0164 [hep-ph]]; Z. B. Kang and J. Soffer, Phys. Lett. B **695**, 275 (2011) [arXiv:1003.4913 [hep-ph]]; Z. B. Kang and J. Soffer, arXiv:1104.2920 [hep-ph].